Modeling, Simulation, and Analysis of Permanent-Magnet Motor Drives, Part I: The Permanent-Magnet Synchronous Motor Drive

PRAGASEN PILLAY, MEMBER, IEEE, AND RAMU KRISHNAN, MEMBER, IEEE

Abstract—**Two types of permanent-magnet ac motor drives are available in the drives industry. These are the permanent-magnet synchronous-motor (PMSM) drive with a sinusoidal flux distribution, and the brushless dc motor (BDCM) drive with a trapezoidal flux distribution. The application of vector control to the PMSM and complete modeling, simulation, and analysis of the drive system are given. State-space models of the motor and speed controller and real-time models of the inverter switches and vector controller are included. Performance differences due to the use of pulsewidth-modulation (PWM) and hysteresis current controllers are also examined. Particular attention is paid to the motor torque pulsations and speed response. Some experimental verification of the drive performance is also given.**

I. Introduction

THE PERMANENT-magnet synchronous motor (PMSM) has numerous advantages over other machines that are conventionally used for ac servo drives. The stator current of an induction motor (IM) contains magnetizing as well as torque-producing components. The use of the permanent magnet in the rotor of the PMSM makes it unnecessary to supply magnetizing current through the stator for constant air-gap flux; the stator current need only be torque-producing. Hence for the same output, the PMSM will operate at a higher power factor (because of the absence of magnetizing current) and will be more efficient than the IM. The conventional wound-rotor synchronous machine (SM), on the other hand, must have dc excitation on the motor, which is often supplied by brushes and slip rings. This implies rotor losses and regular brush maintenance, which implies downtime. Note that the key reason for the development of the PMSM [1] was to remove the foregoing disadvantages of the SM by replacing its field coil, dc power supply, and slip rings with a permanent magnet. The PMSM, therefore, has a sinusoidal induced EMF and requires sinusoidal currents to produce constant torque just like the SM. Current research [2] in the design of the PMSM indicates that it has a higher-torque-to-inertia ratio and power density when compared to the IM or the wound-rotor SM, which makes it preferable for certain high-performance applications like robotics and aerospace actuators. Although present applications tend to be in the fractional to 30-hp range, the feasibility of using the PMSM for up to 125 hp has recently [3] been evaluated.

Most of the earlier research on the PMSM concentrated on its operation from busbar voltages [4], [5]. Damper windings were used to run the machine up to speed on induction motor action with the machine pulling into synchronism by a combination of the reluctance and synchronous motor torques provided by the magnet. During the startup, the magnet exerts a braking torque that opposes the induction-motor-type torque provided by the damper windings. The torque provided by the damper windings must therefore overcome this magnet braking torque, in addition to the load and friction, to run the motor up successfully. The well-established d, q model of the wound rotor synchronous machine is easily adapted to study the performance of a permanent-magnet synchronous motor with damper windings. More recently [6]–[12], the possibility of using the PMSM for servo drives has been examined. It is recognized that with rotor position feedback, the motor can be held in synchronism with the inverter at all times, and the rotor cage [10], [11] is not needed to run the machine up to the commanded speed.

Vector control is normally used in ac machines to convert them, performancewise, into equivalent separately excited dc machines which have highly desirable control characteristics. The application of vector control to the PMSM and its drive system simulation are given in this part of the two-part paper. For high-performance servo drives, hysteresis [3] or PWM current controllers are used to ensure that the actual currents flowing into the motor are as close as possible to the sinusoidal references. This paper evaluates the use of hysteresis as well as PWM current controllers when used in the PMSM drive. Complementary switching of the inverter power devices is considered undesirable and not implemented. In this evaluation, the entire nonlinear drive system is simulated, including the nonlinear d, q axis equations of the motor, state-space model of the speed controller [12], and real-time models of the inverter switches and vector controller. Although the switches are assumed to be ideal, the simulation software developed is flexible enough to accommodate their turn-on and turn-off

Paper IPCSD 88-22, approved by the Industrial Drives Committee of the IEEE Industry Applications Society for presentation at the 1987 Industry Applications Society Annual Meeting, Atlanta, GA, October 19-23. Manuscript released for publication July 12, 1988.

P. Pillay is with the Department of Electrical and Electronic Engineering, University of Newcastle-upon-Tyne, Merz Court, Newcastle-upon-Tyne, England NE1 7RU.

R. Krishnan is with the Electrical Engineering Department, Virginia Polytechnic Institute and State University, Blacksburg, VA 24061.

IEEE Log Number 8825302.

0093-9994/89/0300-0265$01.00

times. Every instant of a power switch opening or closing is simulated to predict accurately the stator current changes and resulting torque pulsations. The effects of changing the magnitude of the hysteresis windows on the motor torque pulsations, the inverter switching frequency, and drive performance are evaluated. In addition, a comparison between the PWM and hysteresis current controllers, based on the previous criteria, is also made. Finally, both the small and large signal behavior of the drive are evaluated. These results can be used to evaluate the drive dynamics for application considerations [13]. Key results are verified experimentally.

The paper is organized as follows. Section II presents the mathematical model of the PMSM. Using this model, vector control of the PMSM is developed in Section III. The operation of the current controllers used in high-performance servo drives are discussed in Sections IV and V while the structure of the entire drive system is explained in Section VI. Sections VII and VIII have the results and conclusion, respectively.

II. Machine Model

The stator of the PMSM and the wound rotor SM are similar. The permanent magnets used in the PMSM are of a modern rare-earth variety with high resistivity, so induced currents in the rotor are negligible. In addition, there is no difference between the back EMF produced by a permanent magnet and that produced by an excited coil. Hence the mathematical model of a PMSM is similar to that of the wound rotor SM. The following assumptions are made in the derivation.

1) Saturation is neglected although it can be taken into account by parameter changes.
2) The induced EMF is sinusoidal.
3) Eddy currents and hysteresis losses are negligible.
4) There are no field current dynamics.
5) There is no cage on the rotor.

With these assumptions, the stator d, q equations of the PMSM in the rotor reference frame are [10]–[12]:

$$v_q = Ri_q + p\lambda_q + \omega_s\lambda_d \tag{1}$$

$$v_d = Ri_d + p\lambda_d - \omega_s\lambda_q \tag{2}$$

where

$$\lambda_q = L_q i_q \tag{3}$$

and

$$\lambda_d = L_d i_d + \lambda_{af}. \tag{4}$$

v_d and v_q are the d, q axis voltages, i_d and i_q are the d, q axis stator currents, L_d and L_q are the d, q axis inductances, λ_d and λ_q are the d, q axis stator flux linkages, while R and ω_s are the stator resistance and inverter frequency, respectively. λ_{af} is the flux linkage due to the rotor magnets linking the stator.

The electric torque is

$$T_e = 3P[\lambda_{af} i_q + (L_d - L_q) i_d i_q]/2, \tag{5}$$

and the equation for the motor dynamics is

$$T_e = T_L + B\omega_r + Jp\omega_r. \tag{6}$$

P is the number of pole pairs, T_L is the load torque, B is the damping coefficient, ω_r is the rotor speed, and J is the moment of inertia. The inverter frequency is related to the rotor speed as follows:

$$\omega_s = P\omega_r. \tag{7}$$

The machine model is nonlinear as it contains product terms such as speed with i_d and i_q. Note that ω_r, i_q, and i_d are state variables.

For dynamic simulation, the equations of the PMSM presented in (1)–(6) must be expressed in state-space form as shown in (8)–(10):

$$pi_d = (v_d - Ri_d + \omega_s L_q i_q)/L_d \tag{8}$$

$$pi_q = (v_q - Ri_q - \omega_s L_d i_d - \omega_s \lambda_{af})/L_q \tag{9}$$

$$p\omega_r = (T_e - T_L - B\omega_r)/J. \tag{10}$$

The d, q variables are obtained from a, b, c variables through the Park transform defined below:

$$\begin{bmatrix} v_q \\ v_d \\ v_0 \end{bmatrix} = 2/3 \begin{bmatrix} \cos(\theta) & \cos(\theta - 2\pi/3) & \cos(\theta + 2\pi/3) \\ \sin(\theta) & \sin(\theta - 2\pi/3) & \sin(\theta + 2\pi/3) \\ 1/2 & 1/2 & 1/2 \end{bmatrix} \cdot \begin{bmatrix} v_a \\ v_b \\ v_c \end{bmatrix}. \tag{11}$$

The a, b, c variables are obtained from the d, q variables through the inverse of the Park transform defined below:

$$\begin{bmatrix} v_a \\ v_b \\ v_c \end{bmatrix} = \begin{bmatrix} \cos(\theta) & \sin(\theta) & 1 \\ \cos(\theta - 2\pi/3) & \sin(\theta - 2\pi/3) & 1 \\ \cos(\theta + 2\pi/3) & \sin(\theta + 2\pi/3) & 1 \end{bmatrix} \begin{bmatrix} v_q \\ v_d \\ v_0 \end{bmatrix}. \tag{12}$$

Note that these transformations apply equally well to currents and flux linkages. The total input power to the machine in terms of the a, b, c variables is

$$\text{power} = v_a i_a + v_b i_b + v_c i_c \tag{13}$$

while in d, q variables,

$$\text{power} = 3(v_d i_d + v_q i_q)/2 \tag{14}$$

for a balanced system.

III. Vector Control of a PMSM

Equations (3) and (4) are represented in a phasor diagram shown in Fig. 1. The rotor flux linkage revolves at rotor speed ω_r and is positioned away from a stationary reference by the rotor angular position, given by

$$\theta_r = \int \omega_r \, dt \tag{15}$$

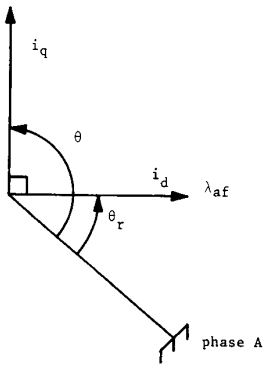

Fig. 1. Phasor diagram of vector controller.

where t is the time. If i_d is forced to be zero, then

$$\lambda_d = \lambda_{af} \tag{16}$$

and

$$T_e = 3P\lambda_{af} i_q / 2. \tag{17}$$

Since the magnetic flux linkage is a constant, the torque is directly proportional to the q axis current. This is represented as

$$T_e = K_t i_q \tag{18}$$

where

$$K_t = 3P\lambda_{af}/2. \tag{19}$$

The torque equation is similar to that of a separately excited dc motor, and this completes the transformation of a PMSM to an equivalent separately excited dc motor. Similarly, the introduction of a negative i_d will weaken the airgap flux as seen from (4).

IV. Hysteresis Current Controller

The power circuit that drives the PMSM is shown in Fig. 2. It is assumed that a reasonably well-filtered dc supply is available. The six switches $T1$–$T6$ are used to control the three stator phase currents. The control strategy is as follows.

The actual values of i_a and i_b that are flowing into the motor are measured. From this i_c can be constructed; this removes the need for an additional current sensor. The actual and reference values are compared and error signals generated. In making the comparison between the actual currents and the reference values, the scheme in Fig. 3 is used. Fig. 3 shows the reference value i_a^*. In addition, two other curves consisting of $i_a^* + \Delta i$ and $i_a^* - \Delta i$ are shown. Δi defines the hysteresis bands. The hysteresis property allows the actual value of i_a to exceed or be less than the reference value by Δi. The logic is shown in Table I. Similar logic applies to the other two phases. Note that complementary switching of the power devices is considered undesirable and, therefore, is not used.

Whenever $T1$ is "on," i_a increases positively using either the B or C phases as a return path. As soon as $T1$ switches from an "on" to an "off" position, and since the current through the machine winding cannot go to zero instantaneously, the freewheeling diode across its complementary transistor, in this case $T4$, begins to conduct the phase A current. When this occurs, the voltage of phase A switches from $+V_{dc}/2$ to $-V_{dc}/2$, where the midpoint of the dc supply V_{dc} is taken as the reference. The opposite occurs when $T4$ switches from "on" to "off." A similar procedure exists in the other phases. The reason that this is called a hysteresis controller is that the phase voltage switches to keep the phase currents within the hysteresis bands. The phase currents are, therefore, approximately sinusoidal: the smaller the hysteresis bands, the more closely do the phase currents represent sine waves. Small hysteresis bands, however, imply a high switching frequency, which is a practical limitation on the power device switching capability. Increased switching also implies increased inverter losses.

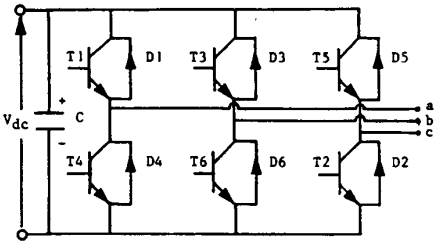

Fig. 2. Inverter circuit of PMSM.

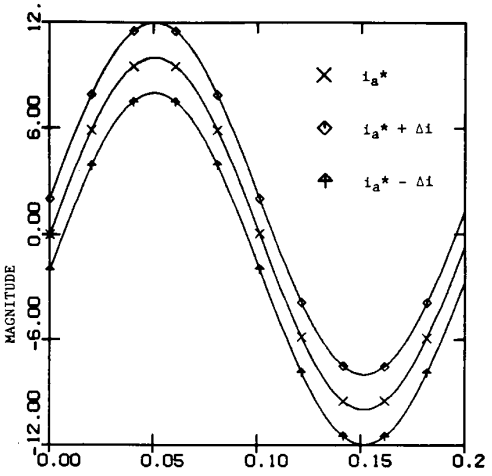

Fig. 3. Hysteresis current controller.

TABLE I

i_a^*	i_a	$T1$	$T4$	V_{on}
≥ 0	$i_a \leq (i_a^* - \Delta i)$	on	off	$+V_{dc}/2$
≥ 0	$i_a \geq (i_a^* + \Delta i)$	off	off	$-V_{dc}/2$ ($D4$ on)
<0	$i_a \geq (i_a^* + \Delta i)$	off	on	$-V_{dc}/2$
<0	$i_a \leq (i_a^* - \Delta i)$	off	off	$+V_{dc}/2$ ($D1$ on)

V. PWM Current Controller

A second method used to generate the required stator currents is to use a pulsewidth-modulated (PWM) current

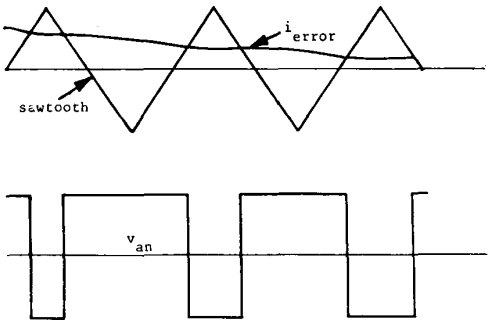

Fig. 4. Pulsewidth-modulated current controller.

controller. The actual values of the three stator currents are measured and compared to the reference currents. Thus error currents are generated. These error currents are compared to a sawtooth-shaped triangular wave as shown in Fig. 4.

If the current error signal is positive and larger than the sawtooth, the voltage is switched positively, while if the current error signal is positive and smaller than the sawtooth, the voltage is switched negatively. Note that it is unnecessary to use complementary switching to achieve this voltage profile.

For example, if $T1$ is conducting, v_{an} is equal to $+V_{dc}/2$, where V_{dc} is the dc supply voltage and the reference is taken as the midpoint of the supply. By switching $T1$ off, the freewheeling diode across $T4$ immediately starts conducting to maintain the current flow through the motor inductance. This automatically forces v_{an} to equal to $-V_{dc}/2$ even though $T4$ is not yet conducting. This is called a PWM current controller because of the pulsewidth modulation of the voltage.

The advantage of the PWM current controller over hysteresis is that the switching frequency is preset, and it is, therefore, easy to ensure that the inverter switching capability is not exceeded. In the hysteresis controller the switching frequency depends on the value of the hysteresis window, and the actual switching frequency demanded from the inverter is unknown. A trial-and-error procedure must be adopted to ensure that the inverter switching frequency is not exceeded. The advantage of the hysteresis over the PWM controller is that, from a control point of view, there is no transportation delay or system lag. In the PWM controller this does exist with the average lag being equal to half the period of the PWM. However, if this lag is less than about one-tenth the stator time constant of the machine, it has a negligible effect on the drive performance.

VI. Drive System

The machine, speed and position feedback, speed and current controllers, and inverter constitute the PMSM drive system as shown in Fig. 5. All reference or commanded values are superscripted with a "*" in the diagram. The error between the reference and actual speeds is operated upon by the speed controller to generate the torque reference. In the constant airgap flux mode of operation where $i_d^* = 0$, the torque reference is divided by the motor torque constant to give the reference quadrature axis current. This goes through the inverse Park transform to generate the a, b, c stator reference currents. Rotor position feedback is needed to generate these currents. The hysteresis or PWM current controller attempts to force the actual motor currents to equal the commanded values at all times. Current feedback is required for the hysteresis or PWM current controllers to achieve this. Current control is implemented by the appropriate firing of power devices $T1$–$T6$ as discussed previously. Both position and speed feedback can be obtained from a resolver/signal processor combination.

When greater than rated speed is commanded, the machine then operates in the constant power or flux-weakening mode. Here, the airgap flux is weakened by applying a direct axis current in opposition to the rotor magnet flux. The torque–speed profile of the drive is as shown in the block labeled FW. The output of the block is unity up to rated speed and decreases hyperbolically with speed between the rated and maximum speeds to ensure constant output power. When the output of FW is unity, then $\lambda_m = \lambda_{af}$ and $i_d^* = 0$. If the output of FW is less than unity, then a lower reference torque is demanded. In addition, λ_m is less than λ_{af} so that a negative i_d^* is commanded to buck the magnet flux. The speed controller is designed at rated speed but is required to operate properly up to the maximum speed.

VII. Results

Digital computer simulations of the entire drive system shown in Fig. 5 are presented in this section. The state-space models of the PMSM and speed controller and switching logic of the current controllers are included in the simulation. Every instant of a power device switching on or off is modeled. The speed controller is a particular case of the pseudo-derivative feedback controller discussed in [12]. Large and small signal transients are considered, and in addition, comparisons between the PWM and hysteresis current controllers are made.

Fig. 6 shows that key transient results when a PMSM (see the Appendix for the parameters) is started up from standstill to a speed of 1750 r/min. A 2-kHz PWM current controller is used. The speed is underdamped in the design used here. The linear manner in which the speed increases is possible because of vector control. During the startup period, the commanded torque equals the maximum capability of the motor. This ensures that the machine runs up in the shortest time possible. From Fig. 6 it is clear that the machine runs up before completing a full current cycle. The phase voltage switches continuously in an effort to force the actual current to equal the commanded value. The close tracking of the commanded current by the actual is evident, except for the initial rise time due to the stator time constant.

At 0.025 s, a load of 1 pu is applied to the motor. This causes a small decrease in the speed as shown in Fig. 6. This decrease is barely perceptible and is less than the speed overshoot that occurred during the startup. The motor electric torque increases to 1 pu to satisfy the load torque requirements.

Fig. 7 shows the corresponding curves when a hysteresis instead of a PWM current controller is used. It is clear that the large signal speed transient is the same as when the PWM

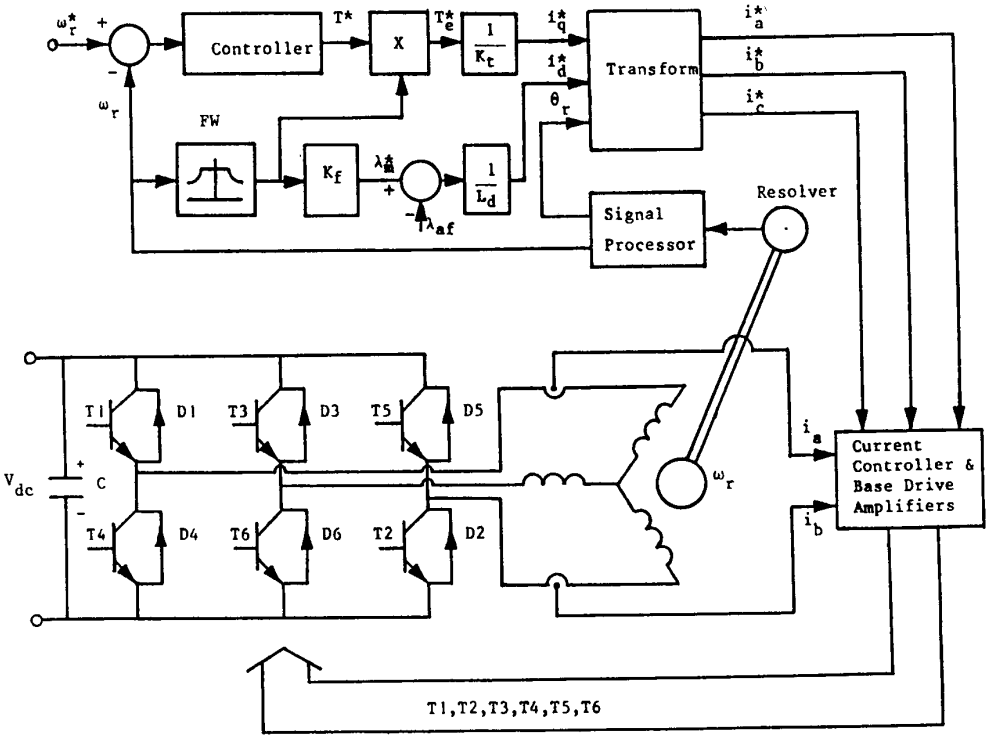

Fig. 5. Schematic of PMSM speed servo drive system.

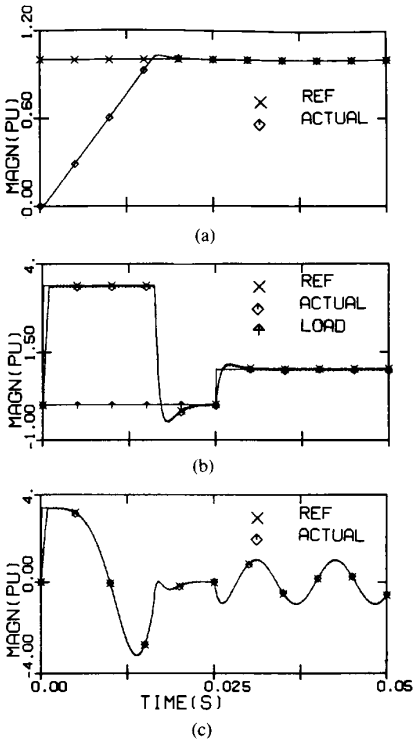

Fig. 6. Transients when fed from PWM CSI. (a) Speed. (b) Torque. (c) Current.

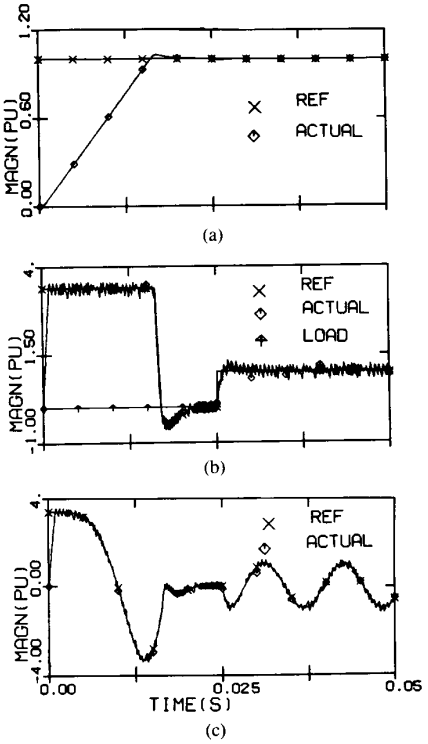

Fig. 7. Transients when fed from hysteresis CSI. (a) Speed. (b) Torque. (c) Current.

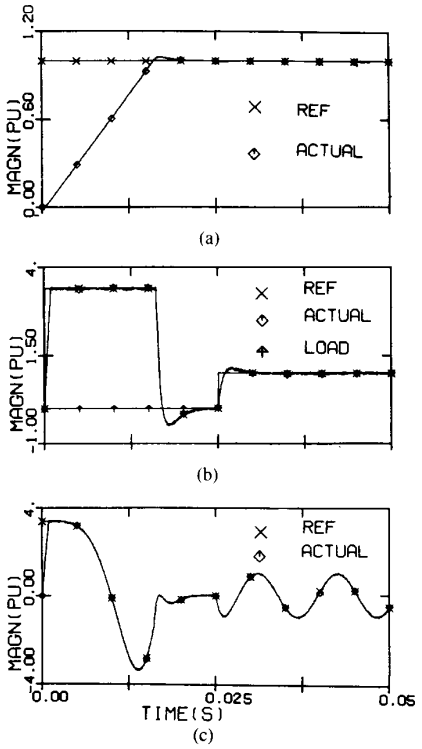

Fig. 8. Transients when fed from hysteresis CSI. (a) Speed. (b) Torque. (c) Current.

current controller is used. However, the actual electric torque in Fig. 7 shows larger instantaneous pulsations than those in Fig. 6. These larger pulsations are produced by the current waveform in Fig. 7. The voltage is used to force the currents to remain within the hysteresis bands. Although the oscillations in the current and, consequently, torque are larger with the hysteresis current controller, the average value of the torque is the same with both current controllers, thus producing the same large-signal dynamics. Lower current oscillations, and hence torque pulsations, are produced by decreasing the size of the hysteresis bands as shown in Fig. 8. This is achieved at a higher switching frequency of the inverter. The linear manner in which the speed increases during the initial startup and subsequent underdamped response are evident.

It is therefore clear that the speed transient is similar irrespective of whether a PWM or hysteresis current controller is used. However, if the hysteresis bands are so large as to produce large-magnitude and low-frequency torque pulsations, then significant speed pulsations would occur.

The torque and current responses when a load torque of 0.1 pu is applied are shown in Fig. 9. These are scaled-down versions of the curves corresponding to the load torque of 1 pu. This indicates that when vector control is used, the large and small signal responses are very similar.

Fig. 10 shows the speed, torque, and current for a 0.1-pu increase in the speed of the machine after it has run up. When the speed command is input, a pulse of torque is demanded to increase the actual speed of the motor. This is provided by an

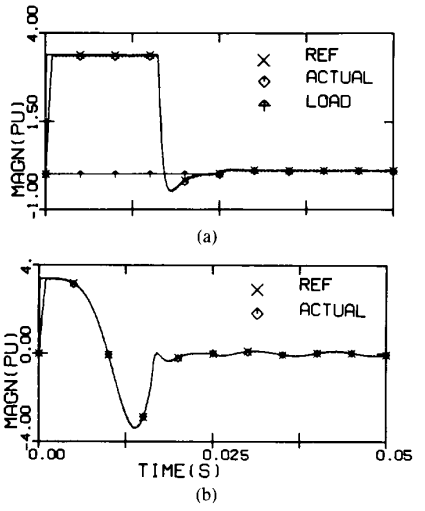

Fig. 9. Transients for 0.1-pu load. (a) Speed. (b) Torque.

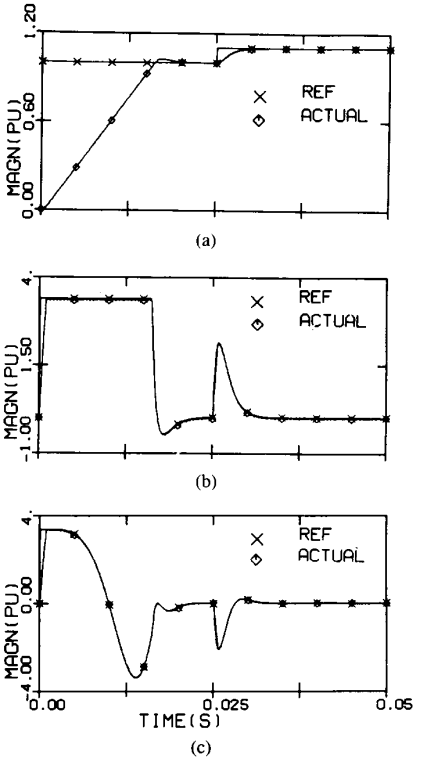

Fig. 10. Transients for 1.1-pu commanded speed. (a) Speed. (b) Torque. (c) Current.

increase in the current as shown in Fig. 10. Up to now transient results have been presented. Steady-state results are presented next.

From the results presented earlier, it is clear that the motor torque pulsations increase as a function of the hysteresis window size. This trend is plotted in Fig. 11 in pu. There is a linear relationship between the magnitude of the motor torque pulsations and the window size. This result was obtained by

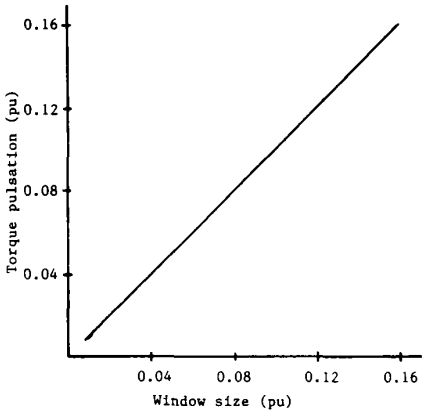

Fig. 11. Torque pulsations versus window size.

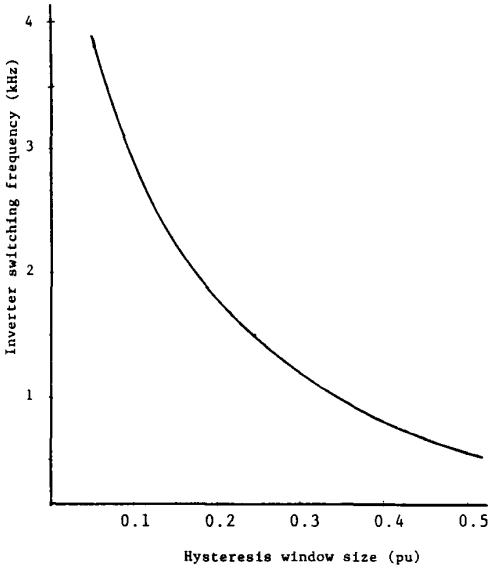

Fig. 12. Inverter frequency versus window size.

varying the hysteresis window size and determining the corresponding torque pulsations. If the window size is expressed in pu with the rms motor stator current as the base, then the pu motor torque pulsations are approximately equal to this window size. In other words, multiplication of the pu window size by the rated torque of the motor gives the actual value of the motor torque pulsations in Nm.

From the previous results, it is also clear that the inverter switching frequency increases as the hysteresis window size decreases. This relationship is shown in Fig. 12. As the hysteresis window size decreases, the required inverter switching frequency increases in a nonlinear manner. A tenfold decrease in the window size results in approximately a sevenfold increase in the inverter switching frequency.

It was found that the torque pulsations due to the 2-kHz PWM current controller shown in Fig. 6 were extremely small, and their effect on the speed was not even noticeable. Changing the PWM switching frequency did not affect the torque pulsations as much as varying the window size in the hysteresis current controller. Hence the results indicate that the PWM switching frequency should be chosen on the basis of the torque bandwidth and inverter switching capability rather than on the resulting torque pulsations.

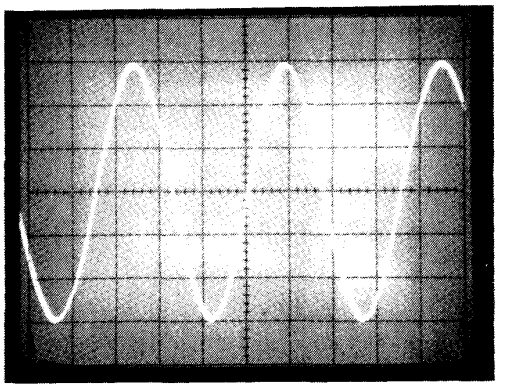

Fig. 13. Back EMF of PMSM. *X* axis: 5 ms/div. *Y* axis: speed (pu).

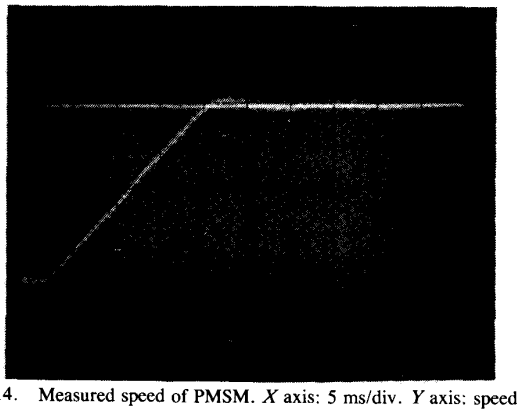

Fig. 14. Measured speed of PMSM. *X* axis: 5 ms/div. *Y* axis: speed (pu).

Experimental Verification

Fig. 13 shows the back EMF of the PMSM, thus verifying that it is sinusoidal. To test the model developed, the machine was started up and its speed measured as shown in Fig. 14. The theoretical prediction of this speed is given in Fig. 15. The theoretical prediction and the practical measurement compare favorably, thus verifying that the model and computer simulation program used in this investigation is valid for the machine used.

VIII. Conclusion

This paper has presented the modeling, simulation, and analysis of a vector-controlled PMSM drive. A systematic derivation of the vector controller for the PMSM was given. The performance differences due to both PWM and hysteresis current controllers were examined.

Since vector control transforms the PMSM to an equivalent separately excited dc machine, the transfer function between the electric torque and current is linear. The results therefore indicate that the small- and large-signal responses are very similar. This result is not true for ac machines that are not under vector control since then the model is nonlinear. The large- and small-signal speed response is the same whether

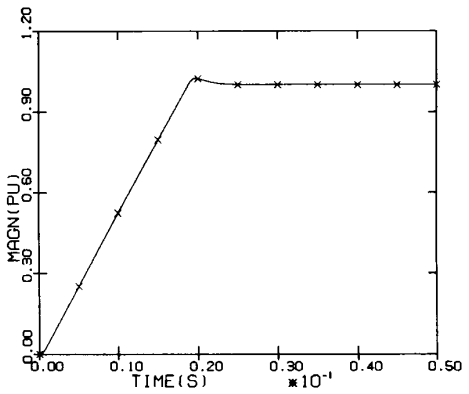

Fig. 15. Predicted speed of PMSM.

PWM or hysteresis current controllers are used. This is because, even though the torque pulsations may be different due to the use of different current controllers, the average value, which determined the overall speed response, is the same.

The larger the hysteresis bands, the lower the inverter switching frequency and the larger are the motor torque pulsations. A PWM switching frequency of 2 kHz produces approximately the same torque pulsations as a hysteresis current controller switching at 3.8 kHz. From this point of view the PWM is better. However, the PWM can have a delay of up to one period corresponding to its carrier frequency. This may have implications in very high speed applications. However, if this delay is less than one-tenth of the stator time constant, it has been found in practice that it has a negligible effect on the drive performance.

The motor torque pulsations are related linearly to the size of the hysteresis bands. If the window size is expressed in pu with the rms value of the motor rated current as the base, then the pu torque pulsations are approximately equal to this pu window size.

Nomenclature

B	Damping constant, N·m/rad/s.
i_a, i_b, i_c	a, b, and c phase currents, A.
i_d, i_q	d and q axis stator currents, A.
J	Moment of inertia, kg·m^2.
L_d, L_q	stator d, q inductances, H.
p	Derivative operator.
P	Number of pole pairs.
R	Stator resistance, Ω.
T_e	Electric torque, N·m.
T_L	Load torque, N·m.
v_d, v_q	d and q axis stator voltages, V.
V_{dc}	DC bus voltage, V.
ω_r	Rotor speed, rad/s.
ω_s	Synchronous speed, rad/s.
λ_{af}	Mutual flux linkage between rotor and stator due to magnet, Wb·turn.
λ_d, λ_q	Stator d and q axis flux linkage, Wb·turn.
λ_m	Air gap flux linkage, Wb·turn.
θ	Angle between stator phase A and the q axis, rad.
θ_r	Angle between stator phase A and the d axis, rad.
*	Superscript indicating reference value.

Appendix
Motor Parameters

We have the following:

$$R = 1.4 \quad \Omega$$
$$L_d = 6.6 \quad \text{mH}$$
$$L_q = 5.8 \quad \text{mH}$$
$$J = 0.00176 \quad \text{kgm}^2$$
$$B = 0.00038818 \quad \text{Nm/rad/s}$$
$$\lambda_{af} = 0.1546 \quad \text{V/rad/s}$$

6 poles.

Acknowledgment

The authors acknowledge Industrial Drives, Kollmorgen Corporation, of Radford, VA, for the donation of the permanent-magnet synchronous motor drive that was used in this paper.

References

[1] D. P. M. Cahill and B. Adkins, "The permanent magnet synchronous motor," *Proc. Inst. Elec. Eng.*, vol. 109, part A, no. 48, pp. 483-491, Dec. 1962.

[2] R. Krishnan and A. J. Beutler, "Performance and design of an axial field permanent magnet synchronous motor servo drive," in *Proc. IEEE Ind. Appl. Soc. Annu. Meeting*, 1985, pp. 634-640.

[3] E. Richter, T. J. E. Miller, T. W. Neumann, and T. L. Hudson, "The ferrite PM ac motor—A technical and economic assessment," *IEEE Trans. Ind. Appl.*, vol. IA-21, no. 4, pp. 644-650, May/June 1985.

[4] V. B. Honsinger, "Permanent magnet machines: Asynchronous operation," *IEEE Trans. Power App. Syst.*, vol. PAS-99, no. 4, pp. 1503-1509, July/Aug. 1980.

[5] T. J. E. Miller, "Transient performance of permanent magnet machines," in *Proc. Ind. Appl. Soc. Annu. Meeting*, 1981, pp. 500-502.

[6] W. Leonard, *Control of Electrical Drives*. New York: Springer-Verlag, 1984.

[7] G. Pfaff, A. Weschta, and A. Wick, "Design and experimental results of a brushless ac servo drive," in *Proc. IEEE Ind. Appl. Soc. Annu. Meeting*, 1982, pp. 692-697.

[8] R. Krishnan, "Analysis of electronically controlled motor drives,"

class notes, Virginia Polytechnic Inst. and State Univ., Blacksburg, 1986.
[9] M. Lajoie-Mazenc, C. Villanueva, and J. Hector, "Study and implementation of hysteresis controlled inverter on a permanent magnet synchronous machine," *IEEE Trans. Ind. Appl.*, vol. IA-21, no. 2, pp. 408–413, Mar./Apr. 1985.
[10] P. Enjeti, J. F. Lindsay, and M. H. Rashid, "Stability and dynamic performance of variable speed permanent magnet synchronous motors," in *Proc. IECON*, 1985, pp. 749–754.
[11] ——, "Parameter estimation and dynamic performance of permanent magnet synchronous motors," in *Proc. IEEE Ind. Appl. Soc. Annu. Meeting*, 1985, pp. 627–633.
[12] P. Pillay and R. Krishnan, "Control characteristics and speed controller design for a high-performance permanent magnet synchronous motor drive," in *Proc. IEEE 1987 Power Electronics Specialists' Conf.*, 1987, pp. 598–606.
[13] ——, "Application characteristics of permanent magnet synchronous and brushless dc motors for servo drives," in *Proc. Ind. Appl. Soc. Annu. Meeting*, 1987, pp. 380–390.

Pragasen Pillay (S'84–M'87) received the B.Eng, M.Sc(Eng), and Ph.D. degrees, all in electrical engineering. The Ph.D. degree was obtained at the Virginia Polytechnic Institute and State University, Blacksburg, while funded by a Fulbright scholarship.

He is currently with the Department of Electrical and Electronic Engineering, University of Newcastle-upon-Tyne, England, UK. His research interests are in the modeling, control, and design of electric motor drive systems.

Dr. Pillay is a past recipient of an IEEE prize award paper. He is a member of the Industry Applications, Industrial Electronics, and Power Engineering Societies of the IEEE and a member of the Industrial Drives Committee of the Industry Applications Society. He is also an Associate Member of the Institution of Electrical Engineers, England, and a member of the Greek honor society, Phi-Kappa-Phi.

Ramu Krishnan (S'81-M'82) received the B.E., M.E., and Ph.D. degrees in electrical engineering.

He taught for seven years in India. He was Staff Engineer and Principal Investigator of ac servo drive projects at Gould Research Center, Rolling Meadows, IL, between 1982 and 1985. Since September 1985 he has been an Associate Professor in the Electrical Engineering Department at Virginia Polytechnic Institute and State University, Blacksburg. His teaching and research interests are in high-performance vector-controlled variable-speed drives, switched-reluctance motor drives, electrical machine design, and static power conversion. He has published more than 50 papers on these topics. He has developed a graduate program in electric motor drives and machine design at Virginia Polytechnic.

Dr. Krishnan is a recipient of four IEEE-IAS awards for his papers, both presented and published. He has been Associate Editor of the IEEE TRANSACTIONS ON INDUSTRIAL ELECTRONICS since June 1987. He is a member of the IAS Machine Tools, Robotics, and Factory Automation Committee.